HAYATI
Journal of Biosciences

Vol. 30 No. 3, May 2023 404-412
DOI:10.4308/hjb.30.3.404-412
ISSN: 1978-3019
EISSN: 2086-4094

Identification of *Vermamoeba vermiformis* and *Tetramitus* sp. Isolated from the Gills of *Oreochromis* sp. (Red Hybrid Tilapia)

Wan NorNadhirah Wan Noor Azmi[1], Fatimah Hashim[1*], Zarizal Suhaili[2,3], Suzana Misbah[1], Nor Hafizah Zakaria[4]

[1]*Biological Security and Sustainability Research Group, Faculty of Science and Marine Environment, Universiti Malaysia Terengganu, Terengganu, Malaysia*
[2]*East Coast Environmental Research Institute, Universiti Sultan Zainal Abidin, Gong Badak Campus, Terengganu, Malaysia*
[3]*Holistic Students Development Centre, Universiti Sultan Zainal Abidin, Gong Badak Campus, Terengganu, Malaysia*
[4]*Institute of Marine Biotechnology, Universiti Malaysia Terengganu, Terengganu, Malaysia*

ARTICLE INFO

Article history:
Received June 12, 2022
Received in revised form October 27, 2022
Accepted November 11, 2022

KEYWORDS:
Gills,
Oreochromis sp.,
Trophozoite,
Tetratmitus sp.,
Vermamoeba vermiformis

ABSTRACT

This study is the first report of an infestation of amoeba in the gills of asymptomatic *Oreochromis* sp. from the Manir River, Terengganu, Malaysia. The results confirmed the presence of two species of amoeba, *Vermamoeba vermiformis* and *Tetratmitus* sp., based on the 18 ribosomal RNA gene sequences with 99% sequence similarity. Morphological observations using light and scanning electron microscopy supported the findings, demonstrating both amoeba species' specific features and locomotions. In the trophozoite stage, the mean size of *V. vermiformis* in the locomotive form was between 25.55 µm in length and 4.17 µm in width. The mean size of *Tetramitus* sp. was 20.96 µm in length and 8.66 µm in width. The diameter of the cyst for *V. vermiformis* was 4.67 µm and *Tetramitus* sp. was 3.37 µm. *V. vermiformis* was characterized by cylindrical trophozoites and single monopodial morphology. *Tetramitus* sp. showed a limax-type and various cell shapes. Infestation of the amoeba was also confirmed by histopathological observation in the lamella region with distinct amoeba characteristics compared to the lamellae's epithelial tissue. These findings revealed the presence of *V. vermiformis* and *Tetramitus* sp. infestation in the gills of *Oreochromis* sp. and its potential pathogenic activity, whilst the symbiosis interaction in *Oreochromis* sp. is still unidentified.

1. Introduction

Free-living amoeba (FLA) is present in almost all water reservoirs and terrestrial environments (Lee *et al.* 2020). According to the World Health Association (2013), members of the genera *Acanthamoeba*, *Naegleria* and *Balamuthia* are known to infect people and are regarded as medically significant owing to the illness they bring to their hosts. These microorganisms are free-living but become pathogenic when they infect hosts (Fouque *et al.* 2015). *Vermamoeba vermiformis* (formerly *Hartmannella vermiformis*) is widely associated with human diseases and is host to bacteria, which is the primary host to the bacteria that causes Legionnaires disease (Dobrowsky *et al.* 2016). Meanwhile, there is no report yet associated with diseases of other vertebrates, and its presence is rarely reported as a parasite. However, a recent report by Hossain *et al.* (2018) indicated the existence of *Tetramitus* in biofilms from sludge production in wastewater plants. A study on FLA diversity also reported the prevalence of *Tetramitus* in agricultural soil in Burkina Faso (Denet *et al.* 2017).

Fish are susceptible to diseases such as parasitism. They can also serve as ideal hosts for parasites that can be dangerous for consumption. The impact of parasitism may vary depending on the severity and virulence of the parasite that causes fish deaths (Huws *et al.* 2005). *Oreochromis* sp., or red hybrid tilapia, is a popular fish, versatile and tolerant of various aquaculture environments, including brackish or saltwater and pond or cage systems. The gills of *Oreochromis* sp. and skin mucous can be a food source for amoebae, and the gill and skin microbiome can also be a beneficial supply of bacterial cells for

* Corresponding Author
E-mail Address: fatimah.h@umt.edu.my

feeding activities, similar to bacterial biofilms in the environment (Wang and Lu 2016). Amoeba is one of the aquatic pathogens that can cause significant diseases in fish, such as amoebic gill disease (AGD) (Padros and Constenla 2021). This disease is common in countries such as Norway, Australia, Chile, and Scotland, affecting Atlantic salmon, rainbow trout, and Brown trout (Boerlage *et al.* 2020). In Malaysia, knowledge of amoeba infestation in fish, particularly a disease detection method in an early phase, is still lacking. Therefore, this study will provide preliminary findings on amoeba infestation in farmed fish, *Oreochromis* sp., in the Manir River, Terengganu, Malaysia.

The molecular technique provides accurate and rapid information for identifying unknown amoeba species. Diagnostic PCR primers targeting different sequences of the 18S (small subunit) ribosomal RNA gene have been widely utilized to identify and detect fish parasites within the host and environmental specimens (Kuiper *et al.* 2006; Schroeder *et al.* 2001; Wong *et al.* 2004). The identification of the amoebae was supported by morphological analysis using light and scanning electron microscopy (SEM). The effect of the amoeba infestation on fish gills was then examined using a histopathological approach. The findings obtained from this study are essential to identify the unknown fish pathogen in our local aquaculture industry. It is hoped that increasing awareness of fish health status of fish could support our aquaculture industry in developing sustainably to meet future fish demands. This study also increases the collection of information related to microorganisms in freshwater fish in Malaysia, as these data will be beneficial for further research on fish health and disease.

2. Materials and Methods

2.1. Chemicals and Media

2.1.1. Page Amoeba Saline (PAS)

Two stock solutions were prepared as stocks 1 and 2. Stock 1 was prepared by mixing 0.14 g of disodium hydrogen phosphate anhydrous (Na_2HPO_4) and 0.13 g potassium dihydrogen phosphate anhydrous (KH_2PO_4) into 500 ml of distilled water. Stock 2 was prepared by adding 4 mg of magnesium sulfate hydrate ($MgSO_4 \cdot 7H_2O$), calcium chloride 2-hydrate ($CaCl_2 \cdot 2H_2O$), and 0.12 g of sodium chloride (NaCl) and dissolved in 500 ml of distilled water (Fatimah *et al.* 2021).

2.1.2. Phosphate Buffered Saline (PBS)

PBS was prepared by adding 8 g of NaCl, 0.20 g of potassium chloride (KCl), 1.44 g of Na_2HPO_4 and 0.24 g of KH_2PO_4 to 800 ml of distilled water. The pH was adjusted to 7.4, and the solution was topped with distilled water to 1 L.

2.1.3. Microbiological Agars

Nutrient agar (NA) was used to cultivate *Escherichia coli*. The medium was prepared by mixing 14 g of nutrient agar with 500 ml of deionized water and autoclaved at 121°C. The medium was then poured into Petri dishes and kept at 4°C. Non-nutritive agar (NNA) was used in the culture of amoeba. Non-nutrient agar (7.5 g) (Oxoid LII) was dissolved in 500 ml of PAS and autoclaved at 121°C. The agar was then poured into Petri dishes and kept at 4°C.

2.1.4. Heat-killed *E. coli*

The *E. coli* stock was obtained from the Microbiology Laboratory, Faculty of Science and Marine Environment, Universiti Malaysia Terengganu, Malaysia. A fresh stock of *E. coli* was inoculated onto a NA plate and incubated at 37°C overnight. The bacteria were harvested by adding PBS, and the suspension was autoclaved at 121°C for 20 min. Heat-killed *E. coli* was kept at room temperature and later used as a food source for the amoeba (Park 2016).

2.2. Isolation of Amoeba from *Oreochromis* sp. Gills

Fifty *Oreochromis* sp. were collected from a fish farm in the Manir River, Terengganu. Gills were swabbed using sterile cotton buds, and the samples were streaked onto the surface of the NNA plate. Heat-killed *E. coli* was supplied as their source of nutrients. Several subculturing series were performed until a pure culture of a similar type of amoebae cyst was obtained. A small piece of NNA was excised and inoculated onto fresh NNA plates (Dykova *et al.* 2005).

2.3. Molecular Identification of Amoeba

The DNA of the amoeba trophozoites was extracted using the innuPREP DNA Mini Kit (ANALYTIK JENA) according to the protocol. Eluted DNA (2 µl) was used as a template for amplifying amoeba genes by Polymerase Chain Reaction (PCR). The PCR reaction was carried out according to Park (2016) in 50 µl volume using specific primers for

FLA (5'-CGCGGTAATTCCAGCTCCAATAGC-3'-forward primer and 5'-CAGGTTAAGGTCTCGTTCGTTAAC-3'-reverse primer). PCR was carried out based on the following parameters: initial denaturation at 94°C for 7 min, 45 cycles of denaturation at 94°C for 60 s, annealing at 65°C for 60 s, extension at 72°C for 60 s, followed by a terminal extension at 72°C for 10 min. The amplified products were electrophoresed on 0.8% agarose gel and later purified using a Wizard PCR Clean-up purification kit (Promega, USA). The purified PCR products were sent for sequencing at First BASE Laboratories Sdn Bhd, Malaysia. The DNA sequencing results obtained were analyzed using BioEdit Sequence Alignment Editor software and further subjected to identification of the amoeba species using Basic Local Alignment Search Tool (BLAST) software (version 2.2.14) in GenBank, National Center for Biotechnology Information (NCBI) database.

2.4. Morphological Observation of Amoeba by Light Microscope and Scanning Electron Microscope (SEM)

Light microscopy was used to examine the live trophozoites and cysts. The specimens were placed on glass slides and observed using an Olympus microscope connected to a digital camera based on the procedure by Fatimah *et al.* (2021). Next, for SEM, The pure culture of amoeba was transferred to coverslips of a 6-well plate and prepared for SEM analysis following the animal tissue processing guidelines at the SEM Laboratory, Universiti Malaysia Terengganu. Initially, the amoeba was fixed in 2.5% glutaraldehyde in 0.1M sodium cacodylate for 2 h at room temperature, followed by 1% osmium tetraoxide in 0.1M sodium cacodylate. The sample was dehydrated in several concentrations of ethanol ranging from 35 to 100% alcohol at room temperature for 10 min for each repetition. This was followed by drying the specimen in hexamethyldisilazane (HMDS) and mounting it on the specimen stub. The specimen was then coated with gold using an Auto Fine Coater and examined with an analytical scanning electron microscope (model JEOL 6360 LA) (Fatimah *et al.* 2021).

2.5. Processing of *Oreochromis* sp. Gills Tissue for Histopathology

The gills of *Oreochromis* sp. were excised using a clean scalpel. Fresh tissues from amoeba-infected gills were cut in 1 cm^2 and fixed in 10% formalin for 24 h to preserve the tissues. The samples were then dehydrated in several dilutions of ethanol and infiltrated in paraffin wax for 24 h before being embedded in solid paraffin blocks. After solidifying, the blocks were trimmed to achieve even surfaces. At least 5 µm of tissue ribbons were sectioned, and these ribbons were transferred onto glass slides, followed by drying on a hot plate for 24 h. The samples were stained using the hematoxylin and eosin methods and then mounted with distyrene plasticizer xylene (DPX) to preserve the stain before observing it under a light microscope. The structure of the gills was also examined with an Analytical Scanning Electron Microscope (model JEOL 6360 LA) (Fatimah *et al.* 2021).

3. Results

3.1. Molecular Identification of Amoeba

The presence of *Oreochromis* sp. gills was evident through PCR amplification using the established primers. The PCR products exhibited an amplified fragment of approximately 800 bp, suggestive of amoeba in the sample (Figure 1). Further DNA sequencing and BLAST analysis revealed the identity of *Hartmannella vermiformis* and *Tetramitus* sp., corresponding to the partial 18S ribosomal RNA sequences of *Hartmannella vermiformis* strain ECH26 (GenBank accession number JQ271688.1) and *Tetramitus* sp. F8-16 (accession number EF378689.1), respectively. Both DNA sequences exhibited 99% similarity to the matched sequences obtained from GenBank.

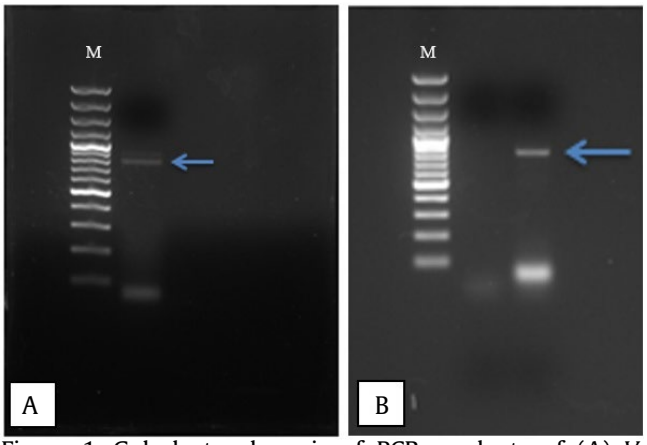

Figure 1. Gel-electrophoresis of PCR products of (A) *V. vermiformis* and (B) *Tetramitus* sp. Both yielded approximately 800bp amplicon sizes (blue arrow). M = 100 bp DNA ladder

3.2. Morphological Morphology Viewed under a Light Microscope

The size and morphological features in the stages of the trophozoites and cysts were recorded in Table 1, Figure 2 and 3. The size of the *V. vermiformis* was found within the scope range, 25.55 µm in length and 4.17 µm in diameter, under the trophozoite stage. The mean size of *Tetramitus* sp. was 20.96 µm in length and 8.66 µm in diameter. Figure 2A showed the presence of a hyaline cap structure during movement, and Figure 2B showed the formation of a cyst. Figure 3A shows the morphology of *Tetramitus* sp. in the trophozoite stage and the formation of a cyst. Contractile vacuole was also observed in *Tetramitus* sp. The active movement showed cylindrical with the presence of a hyaline anterior end, while the posterior end narrowed. The steady movement of *Vermamoeba* species showed slight bulges on one side of the anterior end, but later it turned back to its regular cylindrical state. The flagellate form was not seen in both species.

3.3.Morphological Observation of Amoebae under the Scanning Electron Microscope

SEM micrograph of *V. vermiformis* in the trophozoite form, as shown in Figure 4. *V. vermiformis* shows the presence of a hyaline cap, which can usually be seen during the movement of the cell. It is observed that the posterior end showed uroids, which are used to adhere to the substratum during cell locomotion. The outer characteristic of the cyst shows a smooth layer on the surface.

SEM observation of *Tetramitus* sp. *Trophozoite* shows uroids forming during the cell movement (Figure 5A). Similarly to *V. vermiformis*, the posterior end or uroid is categorized in the non-adhesive origin, resulting from the locomotion relating to the cell's internal processes. These outputs may be either more or less adhesive to the substratum. *V. vermiformis* formed a fasciculate uroid, while *Tetramitus* sp. formed a morulate uroid, also called a rounded uroid, made up of smaller knobs. The size of the *Trophozoite* for *Tetramitus* sp. is smaller than that for *V. vermiformis* because the magnification value was higher, which was 6500×. Meanwhile, from the micrograph (Figure 4B), the sizes of the *V. vermiformis* are larger compared to *Tetramitus* sp. based on the magnification viewed (Figure 5B). It is also noted that the cyst of *Tetramitus* sp. is smooth, and no pores ware observed.

3.4. Histopathological Examination of *Oreochromis* sp. Gills

Haematoxylin and eosin (H and E) staining were performed further to confirm amoeba's presence in

Table 1. Size and diameter of the trophozoite stages of *V. vermiformis* and *Tetramitus* sp.

Species	Trophozoite			Cyst	
	Length (µm)	Range (µm)	Diameter (µm)	Range (µm)	Diameter (µm)
V. vermiformis	25.55±5.282	12.0-37.0	4.17±0.908	4.0-9.5	4.67±0.526
Tetramitus sp.	20.96±4.623	16.0-30.0	8.66±2.236	6.0-18.0	3.37±0.302

Values represent the mean ± SD

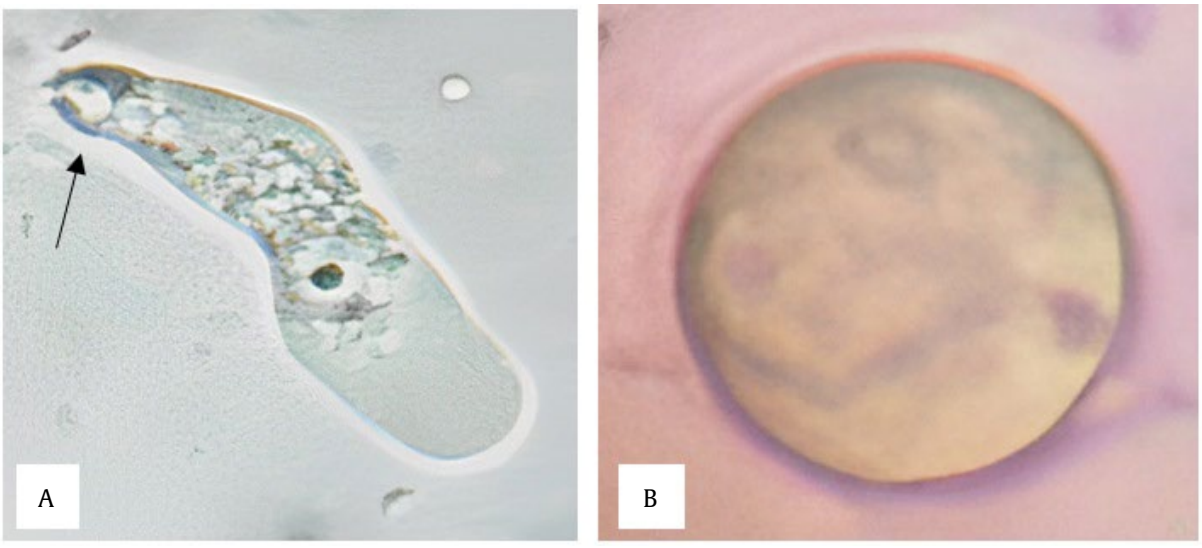

Figure 2. Morphological observation of *V. vermiformis* under a light microscope. (A) The formation of *Trophozoite* shows a hyaline cap (arrow). (B) *V. vermiformis* under cyst stage. The magnifications were 400× for (A) and 1000× for (B)

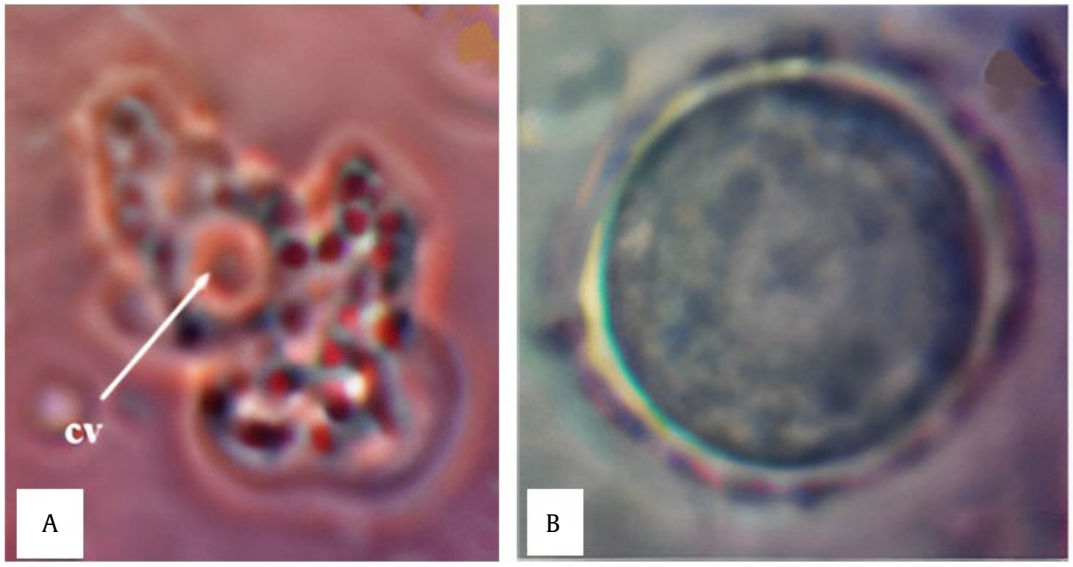

Figure 3. Morphological observation of *Tetramitus* sp. under a light microscope. (A) The formation of *Trophozoite* shows a contractile vacuole (cv). (B) *Tetramitus* sp. in the cyst stage. The magnifications were 400× for (A) and 2500× for (B)

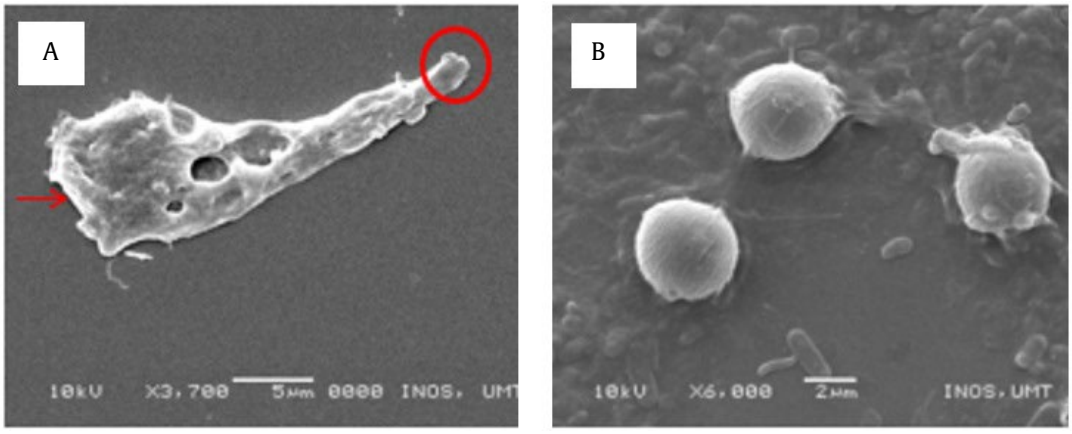

Figure 4. Lower cap for trophozoite (A) and cysts (B) of *V. vermiformis*. The cell contains a hyaline cap (circle) and uroids (arrow). The amplitudes were 3700× for (A) and 6000× for (B)

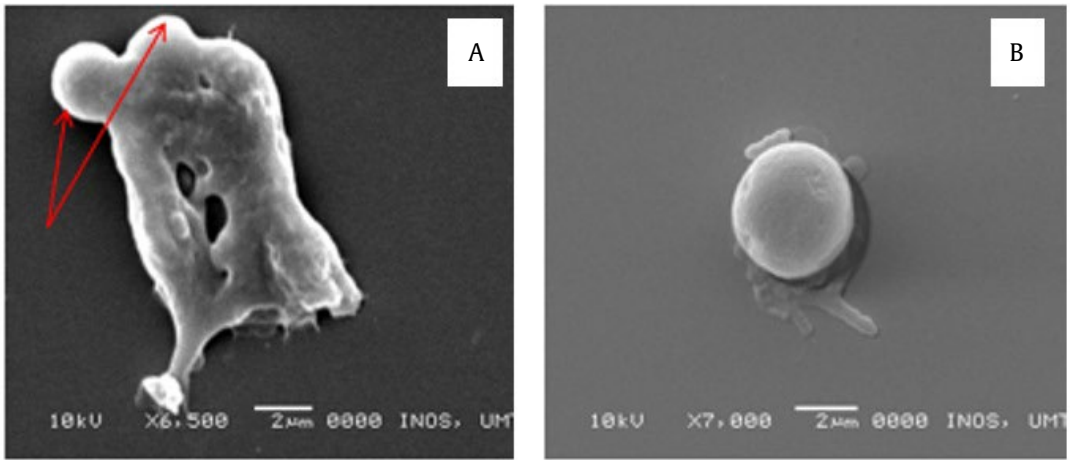

Figure 5. Micrographs of lower cap trophozoite and cysts of *Tetramitus* sp. (A: arrows) Trophozoite with uroidal structure. (B) A smooth surface of the cyst with no pores. Magnification of Micrographs of lower cap trophozoite (6500×) and cyst (7000×)

Oreochromis sp. gill and examine the morphological changes of gill tissues infected by *V. vermiformis* and *Tetramitus* sp. Amoeba was detected to reside on the tip of the primary lamella, as shown in Figure 6A (black arrow). Histopathological data also demonstrated structural changes between the normal and infected gills concerning the lamellae sizes and arrangement. Morphological changes in the gill structure in pillar size and basal cells were also observed in amoeba-infected gills. In the primary lamellae, the infected gills have different structures, and the arrangement of secondary lamellae is perpendicular to the primary lamellae but not organized to each other. Figures 6A and B show that inflammation at the tip of the primary lamellae is observed as one of the results of amoeba infections. Additionally, the presence of amoebae in the gills is seen in pink compared to the lamellar cells after staining with eosin dye.

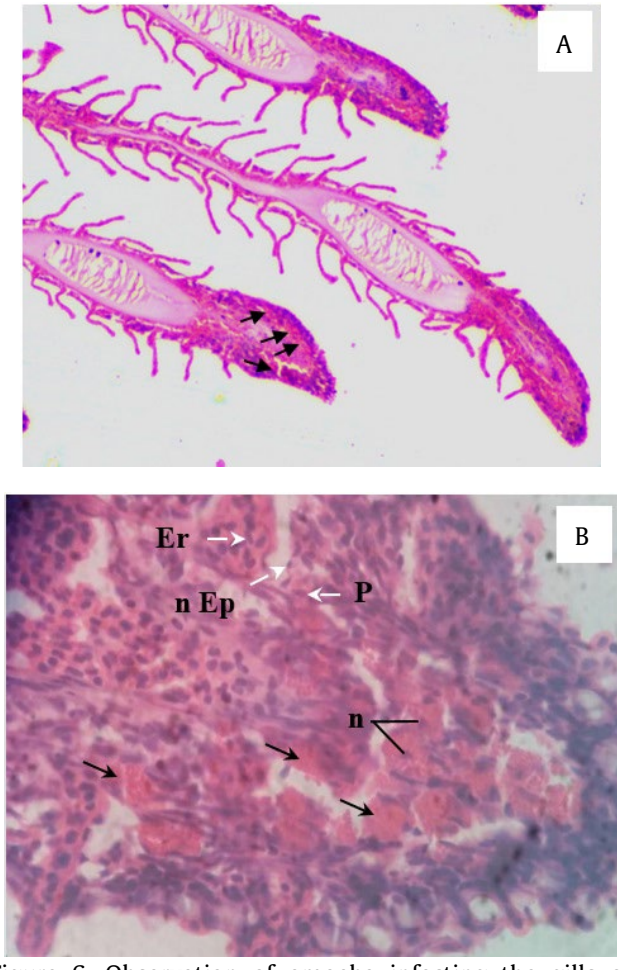

Figure 6. Observation of amoeba infecting the gills of *Oreochromis* sp. (A) Amoeba were present at the tip of primary lamellae (arrows). (B) Detection of amoeba by comparing the size of amoebae (black arrow) with erythrocytes in the lamellae (Er), pillar cell (P) and the nucleus of the epithelial cell (n Ep) on primary lamellae. n: nucleus of amoeba. Magnifications were 50× for (A) and 400× for (B)

3.5. Observation of Amoeba-infected Gills under a Scanning Electron Microscope

In the present study, the gills infected with the amoeba displayed various sizes of the primary lamellae. Only the amoebae at the secondary lamellae were presented for further viewing, as the image of amoebae at the primary lamellae was dented with the epithelial cells. The micrograph of tilapia gill infected with the amoeba by SEM showed changes in the features of secondary lamellae when compared to the normal gill. As shown in Figure 7, the secondary lamellae' appearance differs for the front lamella (a) and (b). The arrangement also is not complete compared to the normal gill.

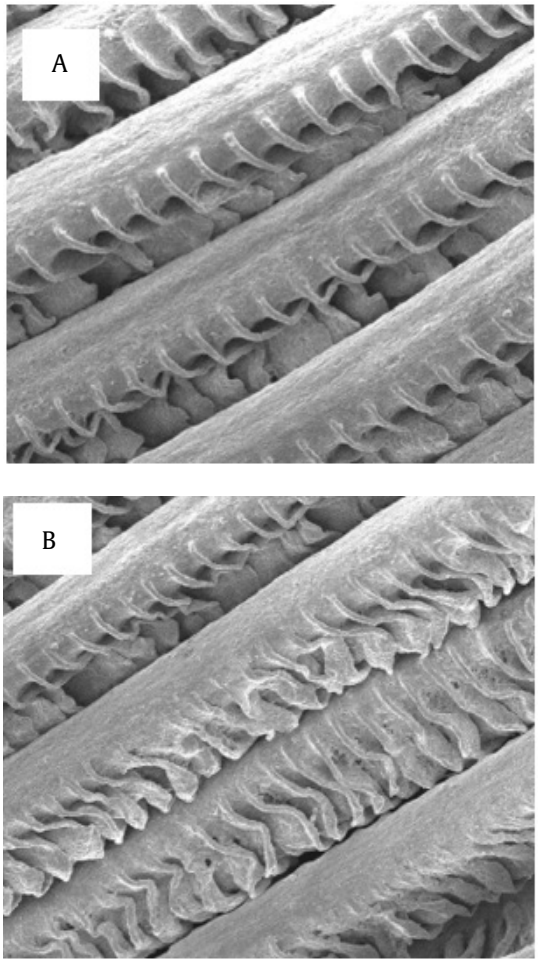

Figure 7. Structure of gills observed under a scanning electron microscope. Arrangement of unorganized secondary lamellae (A) compared to the normal lamellae (B)—100x magnification

4. Discussion

4.1. Molecular Identification of Amoeba

The results of this study confirmed the infestation of amoeba in the gills of *Oreochromis* sp. based on the molecular, morphological, and histological approaches (Page 1986; Smirnov *et al.* 2011). The isolation of amoeba, *V. vermiformis* and *Tetramitus* sp. in this study supports the results of various papers that also outline the isolation of amoeba in the fish gills (Boerlage *et al.* 2020; Dykova *et al.* 2005; Salcedo *et al.* 2009). *Vanella* sp., *Naegleria* sp., *Procanthamoeba* sp., *Acanthamoeba* and *V. vermiformis* sp. also have been observed in the gills of rainbow trout and *Oreochromis* sp. (Dykova *et al.* 2010; Milanez *et al.* 2017). The molecular analysis revealed the amoeba's identity that infected the *Oreochromis* sp. gills based on 18S RNA PCR primers. The application of 18S RNA in identifying *Vermamoeba* has also been reported in other studies (Chelkha *et al.* 2020; Park 2016). This marker is extensively employed in species identification, particularly in microorganisms in complex biological systems such as the gut and environment. It is highly conserved intra-species, facilitating species-level study with high similarities (Wu *et al.* 2015).

4.2. Morphological Description of *V. vermiformis* and *Tetramitus* sp.

The morphological examination of *V. vermiformis* and *Tetramitus* sp. is important to complement its molecular analysis to identify the species accurately. In the present study, observation under the light microscope showed that the size of the amoeba cell varied between *V. vermiformis* and *Tetramitus* sp. The sizes were similar, according to the amoeba guideline that Smirnov and Brown (2004) classified. Cyst formation in amoeba was observed, which could be due to factors such as temperature, pH, and cell concentration. According to Fouque *et al.* (2014), when environmental conditions were not optimal with the cells, encystment took place. During the cyst stage, the cells were smaller than under the trophozoite stage and developed a spherical shape with one or more cell wall layers. In a previous study, the *V. vermiformis* strain formed a spherical or slightly ovoidal shape with smooth-walled walls ranging from 5.1 to 10 µm (Park 2016). The flagellate of the cultured amoeba was not detected, probably due to the inability to produce flagella. Park (2016) reported a similar finding by Park (2016), who observed that no flagellate was formed in the liquid culture and on a solid plate of *V. vermiformis* isolated from a freshwater pond in Korea.

Generally, the amoeba movement is one of the important indications in identifying the species, in addition to the morphological features (Kudryavtsev *et al.* 2022). Smirnov and Brown (2004) mentioned that the first step in species identification is observing the locomotive behavior of moving amoebae under optimum conditions. As shown in the present study, the continuous movement of *V. vermiformis* showed the appearance of a hyaline cap full stop. Smirnov and Brown (2004) stated in their study that the hyaline cap usually exists as the anteroposterior deep as extensive, which occurs in continuous locomotion of the cell. Compared to other species, *Vermamoeba* sp. hyaline cap formation is similar to the genus *Saccamoeba*, but the hyaline cap in *Saccamoeba* is usually reduced with rapid advancement (Smirnov and Brown 2004). Page (1974) suggested that the formed bulges are not distinctly eruptive; along the side, the hyaloplasm also does not run posteriorly. *V. vermiformis* was different from *Leptomyxidae*, which erupted. The locomotion of *Tetramitus* sp. observed under a light microscope also showed eruptive cell movement. A large contractile vacuole was found in the anterior part of the cell in *Tetramitus* sp., followed by smaller extended ones. The trophozoite of *Tetramitus* sp. actively moved during the change in direction. Generally, the amoeba is driven by lobose pseudopodia, which may not be drawn before forming new ones (Anderson 2017).

The morphology of the amoeba was also confirmed under the scanning electron microscope. During observation, there was a large formation of cysts, but it was difficult to see the trophozoite form of the amoeba cell. The cyst formed under several circumstances, such as osmotic stress or chemical treatment (Lambrecht *et al.* 2017). Amoebae have several uroidal structures, such as bulbous, morulate, spineolate, uroidal filaments or collopodium (Smirnov and Brown 2004). In this study, *V. vermiformis* was observed to have a fasciculate uroidal structure, while *Tetramitus* sp. formed a morulate uroid. The bleb-like forms of the cysts of *V. vermiformis* and *Tetramitus* in this study were smooth, and this was supported by some researchers in their studies, who stated that the cyst of *Vermamoeba* is smooth with spherical or ovoid shape (Park 2016).

4.3. Histological Observation of Amoeba in the Gill *Oreochromis* sp.

The amoeba infection in the *Oreochromis* sp. gill was examined by histological technique and further confirmed using the scanning electron microscope. The micrograph showed that the arrangement of the gill was not complete compared to that of the healthy gill. According to Al-Attar (2007), a normal gill is complete in arrangement, and the sizes and structures of the lamellae are similar. The fish gills are easily accessible to surrounding pathogens (Pratte *et al.* 2018). Irritation of the gills caused by infection with pathogens can cause respiratory failure and osmoregulatory complications in fish (Padrós and Constenla 2021). The anatomy of fish gills includes the arch of the gills, primary lamellae, and secondary lamellae, which are perpendicularly arranged with primary lamellae. Some essential cells can be seen in the healthy gills through histology observation, such as red blood cells, epithelial cells, and chloride cells. Chloride cells are usually more circular than epithelial cells and usually at the base of lamellae.

Meanwhile, pilaster cells support the epithelial and mucous cells (Movahedinia *et al.* 2012). However, in this study, only on epithelial cells and erythrocytes morphological changes were detected as there when the gills were infected with the amoeba. The morphological changes observed on histological examination could be the initial sign of disease (Gurcan *et al.* 2009). As Nylund *et al.* (2011) suggested, the early stage of amoeba infection is indicated by the necrotic condition of the epithelial cells and the fusion of the secondary lamellae in the fish gills.

The molecular approach successfully identified the presence of two species of amoebae, *V. vermiformis* and *Tetramitus* sp., using 18s RNA primers. A further histopathological examination confirmed the occurrence of amoeba infestation in the gills of *Oreochromis* sp. Furthermore, morphological characterization related to their particular features and locomotion supported the findings, indicating the potential infestation or commensal relationship of these amoeba species in the Malaysian local fish farm. Further research is needed to detect and prevent amoeba infection in an early rearing stage. Pathological observation must also be done efficiently with an expert guide so that early disease prevention or as a carrier for pathogenic bacteria can be worked out.

Conflict of Interest

The authors declare no conflict of interest.

Acknowledgments

The Ministry of Education funded this research in Malaysia through Universiti Malaysia Terengganu under RAGS (Vot: 57115) RAGS/1/2014/ST03/UMT/1. We also would like to thank Mr Muhammad Embong for assisting in histological works and the Institute of Oceanography and Environment (INOS), Universiti Malaysia Terengganu (UMT), for the facilities.

References

Al-Attar, A.M., 2007. The influences of nickel exposure on selected physiological parameters and gill structure in the teleost fish, *Oreochromis niloticus. J. Biol. Sci.* 7, 77-85. https://doi.org/10.3923/jbs.2007.77.85

Anderson, O.R., 2017. Amoebozoan Lobose Amoebae (Tubulinea, Flabellinea, and Others). in: Archibald J., Simpson A., Slamovits C. (Eds.), *Handbook of the Protists*. Springer, Cham. pp. 1279-1309. https://doi.org/10.1007/978-3-319-28149-0_2

Boerlage, A.S., Ashby, A., Herrero, A., Reeves, A., Gunn. G.J., Rodger H.D., 2020. Epidemiology of marine gill diseases in Atlantic salmon (*Salmo salar*) aquaculture: a review. *Rev. Aquac.* 12, 2140–2159. https://doi.org/10.1111/raq.12426

Chelkha, N., Hasni, I., Louazani, A.C., Levasseur, A., La Scola, B., Colson, P., 2020. Vermamoeba vermiformis CDC-19 draft genome sequence reveals considerable gene trafficking including with candidate phyla radiation and giant viruses. *Sci. Rep.* 10, 5928. https://doi.org/10.1038/s41598-020-62836-9

Denet, E., Coupat-Goutaland, B., Nazaret, S., Pélandakis, M., Favre-Bonté, S., 2017. Diversity of free-living amoebae in soils and their associated human opportunistic bacteria. *Parasitol. Res.* 116, 3151-3162. https://doi.org/10.1007/s00436-017-5632-6

Dobrowsky, P.H., Khan, S., Cloete, T.E., Khan, W., 2016. Molecular detection on *Acanthamoeba* spp. *Naegleria* and *Vermamoeba vermiformis* as vectors for *Legionella* spp. In untreated and solar pasteurized harvested rainwater. *Parasitol. Vec.* 9, 539. https://doi.org/10.1186/s13071-016-1829-2

Dykova, I., Pindova, Z., Fiala, I., Dvorakova, H., Machackova, B., 2005. Fish-isolated strains of *Hartmannella vermiformis* Page, 1967: morphology, phylogeny and molecular diagnosis of the species in tissue lesions. *Folia Parasitol.* 52, 295e303. https://doi.org/10.14411/fp.2005.040

Dykova, I., Kostka, M., Wortberg, F., Peckova, H., 2010. New data on aetiology of nodular gill disease in rainbow trout *Oncorhynchus mykiss. Folia Parasitol.* 57, 157e163. https://doi.org/10.14411/fp.2010.021

Fatimah, H., Siti Aisyah, R., Ma, N.L., Rased, N.M., Mohamad, N.F.A.C., Nur Syakinah Nafisa, F., Azila, A., Zakeri, H.A., 2021. *Aspergillus niger* trehalase enzyme induced morphological and protein alterations on *Acanthamoeba* cyst and molecular docking studies. *J. Parasitol. Dis.* 45, 459–473. https://doi.org/10.1007/s12639-020-01332-3

Fouque, E., Trouilhe, M., Thomas, V., Humeau, P., Héchard, Y., 2014. Encystment of Vermamoeba (Hartmannella) vermiformis: Effects of environmental conditions and cell concentration. Exp. Parasitol. 145, 562-568. https://doi.org/10.1016/j.exppara.2014.03.029

Fouque, E., Yefimova, M., Trouilhe, M.C., Quellard, N., Fernandez, B., Rodier, M.H., Thomas, V., Humeau, P., Héchard, Y., 2015. Morphological study of the encystment and excystment of *Vermamoeba vermiformis* revealed original traits. *J. Eukaryot. Microbiol.* 62, 327-337. https://doi.org/10.1111/jeu.12185

Gurcan, M.N., Boucheron, L. E., Can, A., Madabhushi, A., Rajpoot, N. M., Yener, B., 2009. Histopathological image analysis: a review. *IEEE Rev. Biomedic. Engin.* 2, 147–171. https://doi.org/10.1109/RBME.2009.2034865

Hossain, Md.I., Paparini, A., Cord-Ruwisch, R., 2018. Direct oxygen uptake from air by novel glycogen accumulating organism dominated biofilm minimizes excess sludge production. *Sci. Total Envi.* 640–641, 80-88. https://doi.org/10.1016/j.scitotenv.2018.05.292

Huws S.A., McBain A.J., Gilbert P., 2005. Protozoan grazing and its impact upon population dynamics in biofilm communities. *J. Appl. Microbiol.* 2005;98:238–244. https://doi.org/10.1111/j.1365-2672.2004.02449.x

Kudryavtsev, A., Voytinsky, F., Volkova, E., 2022. *Coronamoeba villafranca* gen. nov. sp. nov. (Amoebozoa, Dermamoebida) challenges the correlation of morphology and phylogeny in *Amoebozoa. Sci. Rep.* 12, 12541. https://doi.org/10.1038/s41598-022-16721-2

Kuiper, M.W., Valster, R.M., Wullings, B.A., Boonstra, H., Smidt, H., van der Kooij, D., 2006. Quantitative detection of the free-living amoeba Hartmannella vermiformis in surface water by using real-time PCR. *Appl. Envi. Microb.* 72, 5750–5756. https://doi.org/10.1128/AEM.00085-06

Lambrecht, E., Baré, J., Sabbe, K., Houf, K., 2017. Impact of *Acanthamoeba* cysts on stress resistance of *Salmonella enterica*, *Serovar Typhimurium, Yersinia enterocolitica* 4/O:3, *Listeria monocytogenes* 1/2a, and *Escherichia coli* O:26. *Appl. Environ. Microb.* 83, e00754-17. https://doi.org/10.1128/AEM.00754-17

Lee, D.I., Park, S.H., Baek, J.H., Yoon, J.W., Jin, S.I., Han, K.E., Yu, H.S., 2020. Identification of free-living amoebas in tap water of buildings with storage tanks in Korea. *Kor. J. Parasitol.* 58, 191–194. https://doi.org/10.3347/kjp.2020.58.2.191

Milanez, G.D., Masangkay, F.R., Thomas, R.C., Ordona, M., Bernales, G.Q., Corpuz, V., Fortes, H., Garcia, C., Nicolas, L. C., Nissapatorn, V., 2017. Molecular identification of *Vermamoeba vermiformis* from freshwater fish in lake Taal, Philippines. *Exp. Parasitol.* 183, 201–206. https://doi.org/10.1016/j.exppara.2017.09.009

Movahedinia, A., Abtahi, B., Bahmani, M., 2012. Gill histopathological lesions of the sturgeons. *Asian J. Anim. Vet. Adv.* 7, 710-717. https://doi.org/10.3923/ajava.2012.710.717

Nylund, S., Andersen, L., Sævareid, I., Plarre, H., Watanabe, K., Arnesen, C.E. Karlsbakk, E., Nylund, A. 2011. Diseases of farmed *Atlantic salmon Salmo salar* associated with infections by the microsporidian *Paranucleospora theridion. Dis. Aqua. Org.* 94, 41–57. https://doi.org/10.3354/dao02313

Padrós, F., Constenla, M., 2021. Diseases caused by amoebae in fish: an overview. *Animals*. 11, 991. https://doi.org/10.3390/ani11040991

Page, F.C., 1974. A further study of taxonomic criteria for limax amoebae, with descriptions of new species and key to genera. *Arch Protist.* 16, 149-184.

Page, F.C., 1986. The limax amoebae: fine comparative structure of the Hartmannellidae (*Lobosea*) and further comparisons with the Vahlkampfiidae (*Heterolobosea*). *Protistol.* 21, 361-383.

Park, J., 2016. First record of potentially pathogenic amoeba *Vermamoeba vermiformis* (Lobosea: Gymnamoebia) isolated from a freshwater of Dokdo Island in the East Sea, Korea. *Anim. System. Evo. Diver.* 32, 1-8. https://doi.org/10.5635/ASED.2016.32.1.001

Pratte, Z. A., Besson, M., Hollman, R. D., Stewart, F. J., 2018. The gills of reef fish support a distinct microbiome influenced by host-specific factors. *Appl. Environ. Microbiol.* 84, e00063-18. https://doi.org/10.1128/AEM.00063-18

Salcedo, N., Gonzaga, E., Garuque, R., Jimenes, V., Panes, T., 2009. Detection of common parasites in freshwater fish sold at the Public Market, Kabacan, Cotabato, Philippines. *USMRD J. Read. Tools.* 17, 147e149.

Schroeder, J.M., Booton, G.C., Hay, J., Niszl, I.A., Seal, D.V., Markus, M.B., Fuerst, P.A., Byers, T.J., 2001. Use of subgenic 18S ribosomal DNA PCR and sequencing for genus and genotype identification of acanthamoebae from humans with keratitis and from sewage sludge. *J. Clin. Microb.* 39, 1903–1911. https://doi.org/10.1128/JCM.39.5.1903-1911.2001

Smirnov, A.V., Brown, S., 2004. Guidelines to the method of study and identification of gymnamoebae. *Protistol.* 3, 148-190.

Smirnov, A.V., Chao, E., Nassonova, E.S., Cavalier-Smith, T., 2011. A revised classification of naked lobose amoebae (Amoeobozoa: Lobosa). *Protistol.* 162, 545-570. https://doi.org/10.1016/j.protis.2011.04.004

Wang, M., Lu, M., 2016. Tilapia polyculture: a global review. *Aqua. Res.* 47, 2363-2374. https://doi.org/10.1111/are.12708

Wong, F.Y., Carson, J., Elliott, N.G., 2004. 18S ribosomal DNA-based PCR identification of *Neoparamoeba pemaquidensis*, the agent of amoebic gill disease in sea-farmed salmonids. *Dis. Aqua. Org.* 60, 65–76. https://doi.org/10.3354/dao060065

World Health Organization, 2013. Guidelines for Safe Recreational Water Environments. Free living Microorganisms.

Wu, S., Xiong, J., Yu, Y., 2015. Taxonomic resolutions based on 18S rRNA genes: a case study of subclass copepoda. *PloS One*. 10, e0131498. https://doi.org/10.1371/journal.pone.0131498